Available online at www.sciencedirect.com
SCIENCE DIRECT®
Optics Communications 216 (2003) 127–132
OPTICS COMMUNICATIONS
www.elsevier.com/locate/optcom

Fabrication of a deep polyimide waveguide grating for wavelength selection

Ying-Tsung Lu[a,b,*], Zheng-Lin Yang[b], Sien Chi[a]

[a] *Institute of Electro-Optical Engineering, National Chiao-Tung University, 1001 Ta Hsueh Road, Hsinchu 300, Taiwan, ROC*
[b] *Opto-Electronics and Systems Laboratories, Industrial Technology Research Institute. Bldg. 51, 195-8 Sec. 4, Chung Hsing Road, Chutung 310, Taiwan, ROC*

Received 30 October 2002; received in revised form 12 December 2002; accepted 16 December 2002

Abstract

A deep polyimide waveguide grating with transmission of −21 dB is demonstrated. A simple lithography process is used to fabricate the raised waveguide, including a deeply corrugated holographic grating. To accurately control the grating period, a rotatable optical setup is used to adjust the interference angle for the holographic process. The corrugation fabricated holographically is 80 nm much deeper than that written directly by an electron beam. The waveguide is thus a promising low-cost wavelength selective device that can be applied to metro networks. The design principles of the optimum mode-matching condition and the efficient transmission for such a deep waveguide grating are also discussed in this paper.

Keywords: Bragg reflector; Waveguide grating; Wavelength selection

1. Introduction

The realization of fiber to the home (FTTH) highly depends on the low-cost optical communication devices. The polymeric waveguide potentially satisfies this requirement. Its performance has been shown to be able to compete with that of silica-based devices in some specific applications [1–3]. The polymeric materials with special optical properties for fabricating waveguide devices have also been developed. Hence the fabrication of the polymer-based waveguide Bragg reflector has been reported [4–6]. However, the properties of polymer materials are sensitive to the humidity and temperature of the environment, which thus affect the performance of the waveguide filters.

Polyimide provides excellent electrical and thermal insulation, as well as maximum physical strength, elongation and toughness. This paper demonstrates the fabrication of a deep waveguide grating using positive photosensitive polyimide. Such a waveguide Bragg reflector is fabricated by a simple lithography process incorporated with holographic interference method. The corrugation of

* Corresponding author. Tel.: +886-3-591-7482; fax: +886-3-591-7479.
E-mail address: lit@itri.org.tw (Y.-T. Lu).

0030-4018/02/$ - see front matter
doi:10.1016/S0030-4018(02)02330-1

the holographic grating can be deeply up to 80 nm leading to large index modulation. In contrast with the electron-beam writing method, our fabrication process provides a large-quantity manufacture method for the corrugated waveguide grating, to fulfill the increasing demands of the low-cost WDM and OADM applications in metro networks.

2. Design principle

2.1. Low-loss mode-matching condition

Light can propagate in a raised waveguide [7] with most of its intensity being confined in the fundamental mode, if the input coupling condition between the fiber and the waveguide is well controlled. The allowed vertical mode number of a waveguide as shown in Fig. 1 is [8]

$$m \leqslant \frac{2}{\pi}\left[k_0 \frac{h}{2}\sqrt{n_a^2 - n_s^2} - \frac{1}{2}\tan^{-1}\sqrt{\frac{n_s^2 - n_0^2}{n_a^2 - n_s^2}}\right], \qquad (1)$$

where m represents the mode number and h is the height of the waveguide. The terms n_a, n_s and n_0 are the refractive indices of the polyimide, glass substrate and air, respectively; $k_0 = 2\pi/\lambda_0$ is the wave number, where λ_0 is the wavelength in the air. The mode numbers of the waveguides with various heights are calculated from Eq. (1) and shown in Fig. 2. According to this numerical result, we chose a raised waveguide with a cross-section of 4×4 μm to fabricate the waveguide filter, because it has less mode number and is sufficiently wide to be processed easily by using lithography. To optimize the mode-matching condition for efficient coupling, we use the full vector FDTD beam-propagation method to calculate the fundamental mode energy of the TE propagation inside the waveguide for incident beams with various diameters [9,10]. Here the TE propagation is defined as the propagation with electrical field vector parallel to the y-axis. Fig. 3 presents the ratio of the fundamental mode energy to the total energy inside the 4×4 μm raised waveguide versus different spot sizes of an incident beam. When the incident beam diameter is around

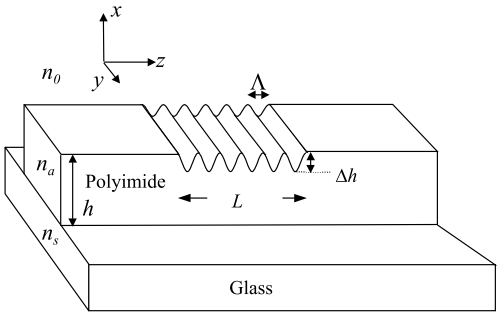

Fig. 1. Schematic structure of the raised waveguide on a glass substrate.

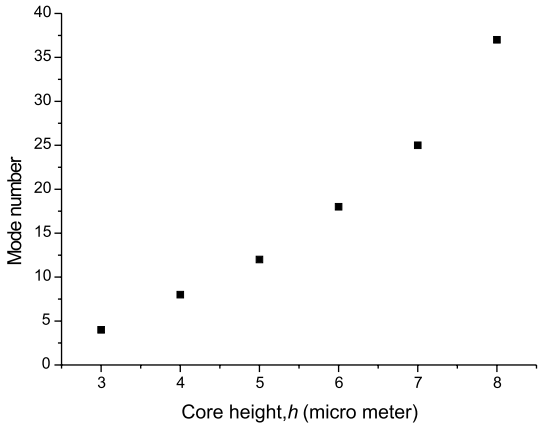

Fig. 2. Vertical mode numbers (black block) versus the height of the waveguide as shown in Fig. 1.

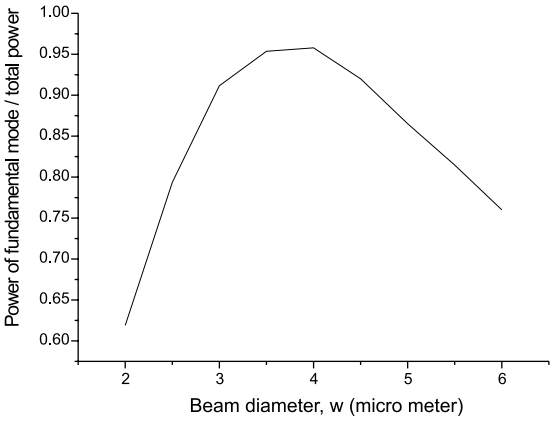

Fig. 3. Ratio of the fundamental mode power to the total power inside the waveguide with a 4×4 μm cross-section versus various input beam diameters.

$w = 4$ μm (full width at e^{-1} magnitude), the waveguide has the largest fundamental mode energy (over 90% of the total energy) to provide the efficient transmission.

2.2. Bragg reflection

The Bragg condition for the reflection of a beam from a waveguide grating with average refractive index n_{av} is

$$2n_{av}k_0 = K, \tag{2}$$

where $K = 2\pi/\Lambda$ is the grating number and Λ is the grating period. For a sinusoidal raised waveguide grating fabricated holographically, as shown in Fig. 1, the perturbation of the dielectric constant can be written as [11,12]

$$\Delta\varepsilon(x,z) = \left[\Delta\varepsilon(x)\frac{\cos(2\pi/\Lambda)z - 1}{2}\right], \tag{3}$$

where

$$\Delta\varepsilon(x) = \begin{cases} \varepsilon_0(n_a^2 - n_0^2), & -\Delta \leqslant x \leqslant 0, \\ 0, & \text{otherwise.} \end{cases}$$

Expanding $\cos(2\pi/\Lambda)z$ as a Fourier series yields the dielectric perturbation

$$\Delta\varepsilon(x,z) = \sum_l \varepsilon_l(x)\exp\left[-\mathrm{i}l\left(\frac{2\pi}{\Lambda}\right)z\right], \quad l = -1, 0, 1, \tag{4}$$

where,

$$\varepsilon_l(x) = \frac{1}{4}\varepsilon_0(n_a^2 - n_0^2), \quad l = \pm 1,$$

$$\varepsilon_l(x) = -\frac{1}{2}\varepsilon_0(n_a^2 - n_0^2), \quad l = 0.$$

Only the Fourier component of $l = 1$ in Eq. (4), i.e., $\varepsilon_1(x) = \frac{1}{4}\varepsilon_0(n_a^2 - n_0^2)$, satisfies the Bragg condition $\beta_B - (-\beta_B) - 1 \times 2\pi/\Lambda = 0$ for the backward coupling. Here β_B is the propagation constant of the fundamental mode at Bragg wavelength. Therefore, the coupling coefficient k_c of the waveguide grating becomes [12]

$$k_c = \frac{\omega}{4}\int_{-\Delta h}^{0} \varepsilon_1(x)|E(x)|^2\,\mathrm{d}x = \frac{\omega}{16}\varepsilon_0\left(n_a^2 - n_0^2\right)\int_{-\Delta h}^{0}|E(x)|^2\,\mathrm{d}x, \tag{5}$$

where Δh is the depth of the grating, and ω is the angular frequency of the input beam. The fundamental TE mode function in the x direction is [12]

$$E(x) = C\left[\cos px - \frac{q}{p}\sin px\right], \tag{6}$$

where $p = (n_a^2 k_0 - \beta_1)^{1/2}$, $q = (\beta_1^2 - n_0^2 k_o^2)^{1/2}$, and C is an arbitrary constant. The forward and backward power flows on the input edge of the waveguide grating can be determined by substituting Eq. (6) into Eq. (5) to estimate the coupling coefficient. By comparing the backward power to the input power, the reflectivity is obtained as [12]

$$R = \frac{|k_c|^2 \sin h^2 sL}{s^2\cos h^2 sL + (\Delta\beta/2)^2 \sin h^2 sL}, \tag{7}$$

where

$$s = \left(k_c^* k_c - \left(\frac{1}{2}\Delta\beta\right)^2\right)^{1/2};$$

$$\Delta\beta = \beta_1 - (-\beta_1) - 2\pi/\Lambda;$$

β_1 is the propagation constant of fundamental mode; and L is the length of the grating. Moreover, the maximum transmission at Bragg wavelength can be written as $T = 1 - R$. Fig. 4 depicts the maximum transmissions with respect to various corrugation depths for various heights of a 10 mm-long waveguide grating. As a result, a waveguide with a cross-section of 4×4 μm in conjunction with an 80-nm depth grating can select a wavelength with a reflectivity of almost 22.5 dB.

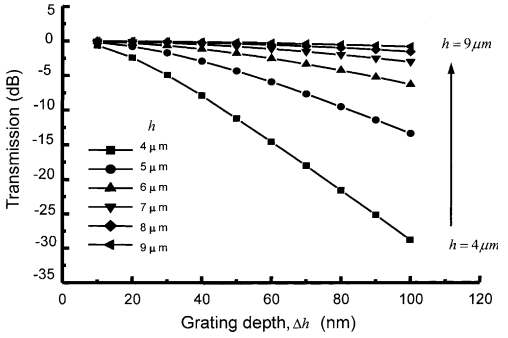

Fig. 4. Simulation of the transmission dip of stop bands versus various grating depths for different waveguide heights.

3. Experiment

In our experiment, a positive photosensitive polyimide (PW-1000 from Toray Co.) was used to fabricate the waveguide Bragg reflector by following the processes illustrated in Fig. 5. The polyimide was spin-coated on a glass substrate (Model B270 from Schott) and then pre-baked 4 min in an oven at 110 °C in flowing nitrogen. The I-line lithography was performed to address the waveguide area on the polyimide according to the photomask pattern under the UV light exposure. The photomask was removed and the two-laser-beam interference was used to expose the holographic grating on the polyimide. By optimizing the dosage of UV exposure and the laser beam interference, the waveguide and holographic grating were constructed simultaneously via development by using a 3% tetramethyl ammonium hydroxide (TMAH) solution. Figs. 6 and 7 present a SEM picture of the waveguide and an atomic force microscope (AFM) picture of the holographic grating with a depth of 80 nm, respectively. Table 1 lists the process parameters associated with the implementing of the waveguide grating.

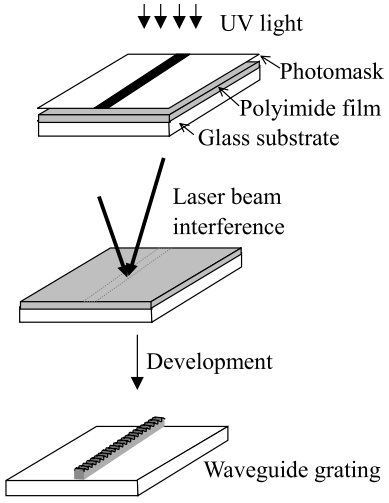

Fig. 5. Fabrication processes for the waveguide Bragg reflector.

Fig. 8 illustrates the tunable optical setup for fabricating grating by the laser beam interference. In our fabrication process, the L-shape holder was rotated around the axis "a" to record a grating with the period

$$\Lambda = \frac{\lambda}{2\sin\theta}, \tag{8}$$

where Λ is the grating period; λ is the wavelength of the laser beam, and θ is the half interference angle. Fig. 9 plots the grating period versus the half interference angle at $\lambda = 442$ nm. By taking the positive value of the differentiation of Eq. (8), the grating period is changed with the resolution of

$$\Delta\Lambda = \frac{1}{2}\lambda\frac{\cos\theta}{\sin^2\theta}\Delta\theta, \tag{9}$$

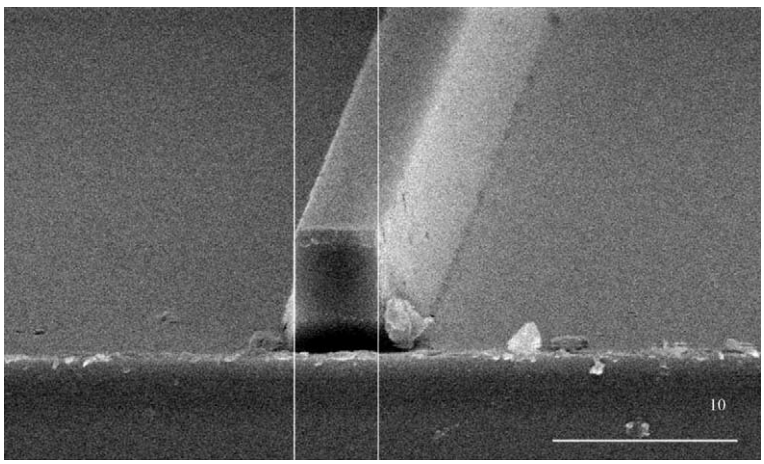

Fig. 6. SEM picture of the polyimide raised waveguide with a 4×4 μm cross-section.

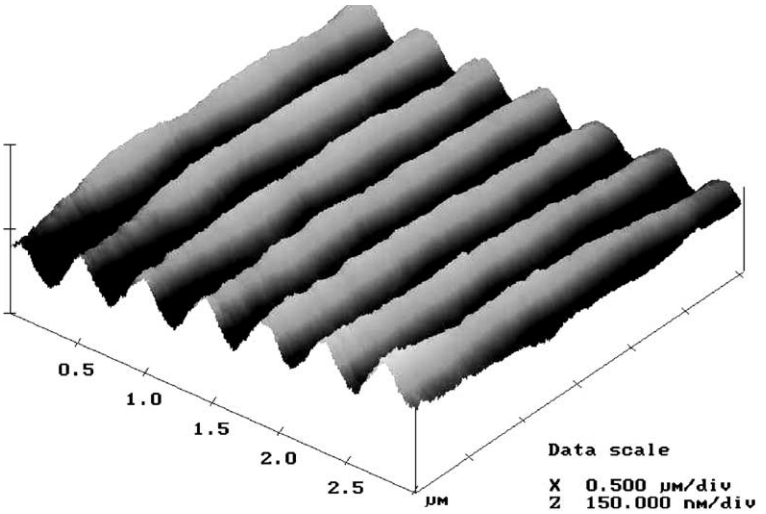

Fig. 7. AFM picture of the holographic grating with a depth of 80 nm.

Table 1
Process parameters for the polyimide waveguide grating

Process items	Parameter
Fabrication of polyimide film	Spin coated with 4000 rpm for 25 s
I-line lithography at 365 nm	146 mJ/cm^2
Laser beam interference at 442 nm	25 mJ/cm^2
Development agent	3% tetramethyl ammonium hydroxide (TMAH) solution
Development time	110 s
Pre-bake before lithography	110 °C, 4 min
Post-bake after development	250 °C, 2 h

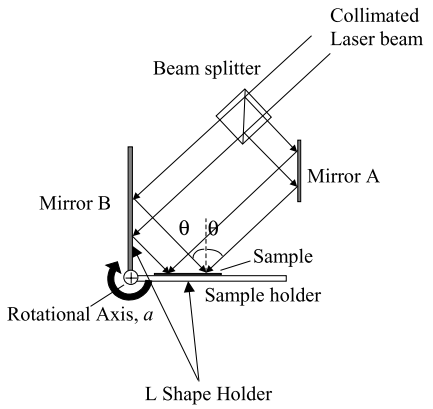

Fig. 8. Tunable optical setup of laser beam interference for fabricating the holographic grating.

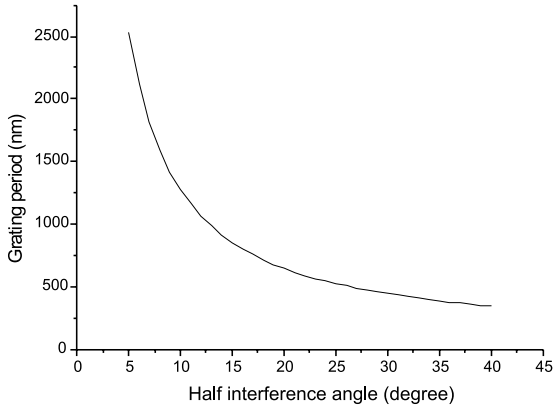

Fig. 9. Simulation of the grating period (Λ) versus the half interference angle (θ) according to the optical setup as shown in Fig. 8.

where $\Delta\theta$ is the rotational resolution of rotation stage. According to Eq. (9), various grating periods can be obtained at a resolution better than 1 nm by using a common stage rotated with a resolution of 0.001 radian to select a wavelength about 1550 nm. A higher resolution can be achieved by adopting a more precise rotational stage. Furthermore, to measure the performance of the waveguide filter, a lens fiber was used to adjust the appropriate spot size of the incident beam onto the edge of the waveguide. Fig. 10 presents the measured stop band with a transmis-

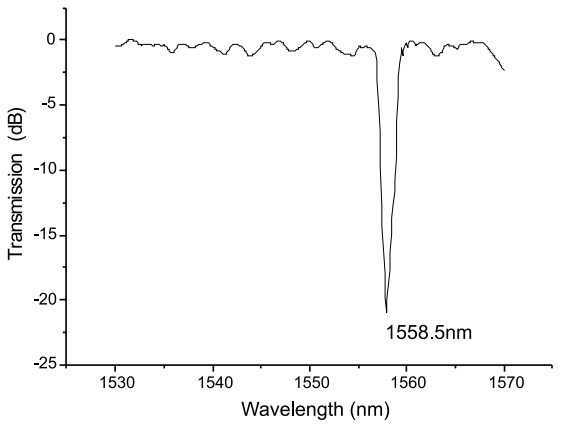

Fig. 10. Measured transmission spectrum of the waveguide Bragg reflector.

sion dip of −21 dB at 1558.5 nm (measured by an OSA with resolution of 0.1 nm) with a 1 dB bandwidth of 1 nm. This holographic grating has a corrugation of 80 nm being much deeper than that of 10 nm written directly by an electron beam in [6]. Consequently, our process provides the large index modulation and thus results in efficient wavelength selection. An insertion loss of 3.6 dB, including the Fresnel reflection, was measured.

4. Conclusion

A deep waveguide grating has been successfully fabricated by using a positive polyimide. By controlling the coupling condition, over 90% of energy can be confined in the fundamental mode resulting in its low-loss transmission. Our fabrication process is a promising low-cost method for fabricating wavelength filters for the applications in local networks. It is also potential to integrate with various silica and polymer components to fabricate advanced devices for optical communication.

References

[1] L. Eldada, L.W. Shacklette, IEEE J. Select. Topics Quant. Electron. 6 (2000) 54.
[2] C.F. Kane, R.R. Krchnavek, IEEE Photon. Technol. Lett. 7 (1995) 535.
[3] C.F. Kane, R.R. Krchnavek, IEEE Trans. Comp., Packag., Manufact. Technol. B 18 (1995) 565.
[4] M.C. Oh, M.H. Lee, J.H. Ahn, H.J. Lee, S.G. Han, Appl. Phys. Lett. 72 (1998) 1559.
[5] W.H. Wong, Z. Zhou, E.Y.B. Pun, Appl. Phys. Lett. 78 (2001) 2110.
[6] W.H. Wong, E.Y.B. Pun, OFC 2002, paper TuC5, 2002, p. 18.
[7] C. Gorecki, in: P.R. Choudhury (Ed.), MEMS and MOEMS Technology and Application, SPIE, 2000, Chapter 5.
[8] K. Okamoto, Fundamentals of Optical Waveguides, Academic, San Diego, 2000.
[9] M.D. Feit, J.A. Fleck Jr., Appl. Opt. 19 (1980) 1154.
[10] W.P. Huang, C.L. Xu, IEEE J. Quant. Electron. 29 (1993) 2639.
[11] A.M. Vengsarkar, P.J. Lemaire, J.B. Judkins, V. Bhatia, T. Erdogan, J.E. Spie, J. Lightwave Technol. 14 (1996) 58.
[12] P. Yeh, Optical Wave in Crystal, Wiley, New York, 1984.